Crystal Phase Quantum Well Emission with Digital Control

Assali, S.; Lähnemann, J.; Vu, TTT; Jöns, K. D.; Gagliano, L; Verheijen, M. A.; Akopian, N.; Bakkers, E. P.A.M.; Haverkort, J. E.M.

DOI
10.1021/acs.nanolett.7b02489

Publication date
2017

Document Version
Final published version

Published in
Nano Letters: a journal dedicated to nanoscience and nanotechnology

Citation (APA)
Assali, S., Lähnemann, J., Vu, TTT., Jöns, K. D., Gagliano, L., Verheijen, M. A., Akopian, N., Bakkers, E. P. A. M., & Haverkort, J. E. M. (2017). Crystal Phase Quantum Well Emission with Digital Control. *Nano Letters: a journal dedicated to nanoscience and nanotechnology*, *17*(10), 6062-6068. https://doi.org/10.1021/acs.nanolett.7b02489

NANO LETTERS

Letter

pubs.acs.org/NanoLett

Crystal Phase Quantum Well Emission with Digital Control

S. Assali,[†,⊥] J. Lähnemann,[‡] T. T. T. Vu,[†] K. D. Jöns,[§,#] L. Gagliano,[†] M. A. Verheijen,[†,∥] N. Akopian,[†,§,▽] E. P. A. M. Bakkers,[†,§] and J. E. M. Haverkort*[,†]

[†]Department of Applied Physics, Eindhoven University of Technology, 5600 MB, Eindhoven, The Netherlands

[‡]Paul-Drude-Institut für Festkörperelektronik, Hausvogteiplatz 5-7, 10117 Berlin, Germany

[§]Kavli Institute of Nanoscience, Delft University of Technology, 2600 GA, Delft, The Netherlands

[∥]Philips Innovation Services Eindhoven, High Tech Campus 11, 5656 AE, Eindhoven, The Netherlands

Supporting Information

ABSTRACT: One of the major challenges in the growth of quantum well and quantum dot heterostructures is the realization of atomically sharp interfaces. Nanowires provide a new opportunity to engineer the band structure as they facilitate the controlled switching of the crystal structure between the zinc-blende (ZB) and wurtzite (WZ) phases. Such a crystal phase switching results in the formation of crystal phase quantum wells (CPQWs) and quantum dots (CPQDs). For GaP CPQWs, the inherent electric fields due to the discontinuity of the spontaneous polarization at the WZ/ZB junctions lead to the confinement of both types of charge carriers at the opposite interfaces of the WZ/ZB/WZ structure. This confinement leads to a novel type of transition across a ZB flat plate barrier. Here, we show digital tuning of the visible emission of WZ/ZB/WZ CPQWs in a GaP nanowire by changing the thickness of the ZB barrier. The energy spacing between the sharp emission lines is uniform and is defined by the addition of single ZB monolayers. The controlled growth of identical quantum wells with atomically flat interfaces at predefined positions featuring digitally tunable discrete emission energies may provide a new route to further advance entangled photons in solid state quantum systems.

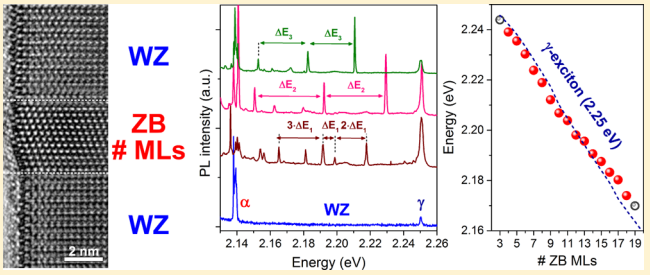

KEYWORDS: *Semiconductor nanowire, gallium phosphide, crystal phase quantum well, spontaneous polarization, photoluminescence*

Quantum confinement of electrons and holes in semiconductors is commonly realized by combining semiconductors with different bandgaps in quantum well (QW) and quantum dot (QD) heterostructures. However, alloy fluctuations and interface roughness prevent a precise control over the emission energy. Consequently, fine-tuning of each individual QD emission energy is required by using the Stark effect or strain methods,[1−4] which severely limits the use of heterostructures as identical single-photon emission sources in photonic circuits.[5] To overcome these limitations, homojunctions made of zinc blende (ZB) and wurtzite (WZ) crystal phases can be grown with a high degree of control in semiconductor nanowires (NWs).[6−9] This method allows the fabrication of atomically sharp crystal phase quantum well (CPQW) and quantum dot (CPQD) structures with monolayer thickness control, allowing digitally tuning of the emission wavelength.[10] In this type of homojunctions, the band offset between the WZ and ZB phases results in carrier confinement within the WZ phase at either side of the ZB barrier[7,11−14] while avoiding residual strain and alloy intermixing as in the case of compositional heterojunctions. We will refer to this novel charge confinement structure as a CPQW. Due to the atomically flat confinement potentials in these CPQWs, the line width of the QW emission can be significantly reduced as compared to a compositional QW. Optical emission from confined states in CPQWs with different charge confinement geometries has been shown in InP and GaAs nanowires,[8,10,11] where the emission of single-photons and cascaded photon-pairs was demonstrated.[15]

Recently, highly reproducible crystal-phase switching was shown in GaP nanowires, with a control over the ZB segment length approaching the monolayer (ML) level.[6] In this material system, the ZB phase has an indirect band gap,[16,17] while a quasi-direct band gap is observed in the WZ phase, promising a route to single-photon emission in the visible spectral range.[18−20] In addition, strong spontaneous polarization fields across the WZ/ZB/WZ segments are predicted for GaP.[21] The discontinuity of the spontaneous polarization P_{SP} induces polarization sheet charges at the WZ/ZB/WZ interfaces,[22] resulting in the quantum-confined Stark effect (QCSE) where the carrier confinement is determined by the polarization-induced triangular potentials.[23,24] Since the ZB barrier is atomically flat, the separation between the positively and the negatively charged carrier sheets is precisely defined, thus avoiding any broadening effects due to spatial inhomogeneities in the electrostatic and confinement potentials. This behavior has been investigated in

Received: June 13, 2017
Revised: September 6, 2017
Published: September 11, 2017

DOI: 10.1021/acs.nanolett.7b02489
Nano Lett. 2017, 17, 6062−6068

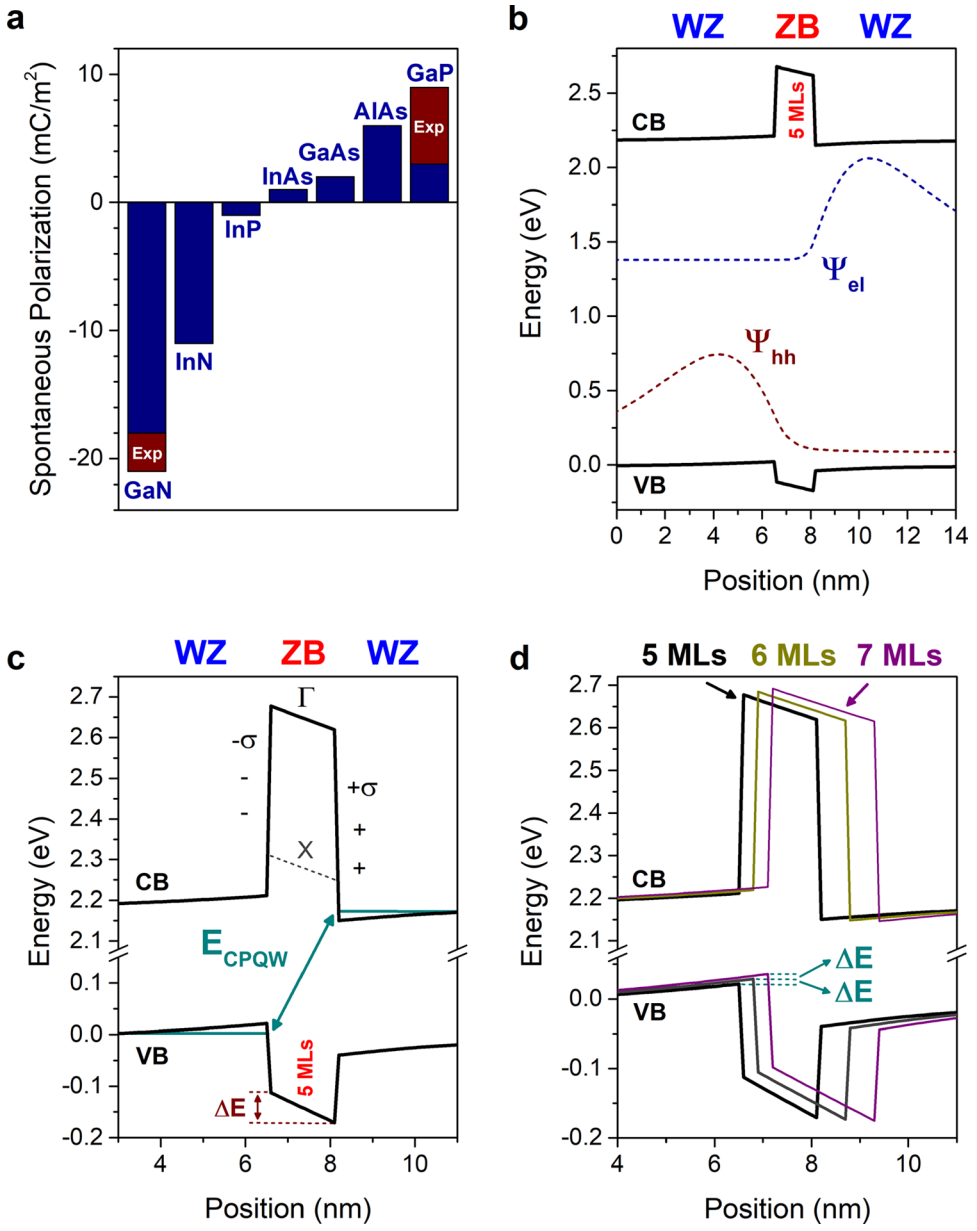

Figure 1. (a) Plot of the spontaneous polarization fields in III−V semiconductors. The dark blue areas are the values predicted from DFT, while the dark red areas are the values determined from experimental measurements. (b) Calculated band diagram for a CPQW in GaP with 5 ZB MLs using 1D Schrödinger−Poisson simulations. The dashed lines indicate the normalized wave functions for electrons (dark blue) and holes (dark red). Curves are shifted to allow easier comparison. (c) Enlarged view of panel b showing a capacitor-like charge configuration where the sheet of polarization charges and the related QCSE are sketched. (d) Digital tuning of the CPQW transition energy for increasing ZB thicknesses of 5, 6, and 7 MLs. By adding (removing) one monolayer, the resulting transition will be decreased (increased) by an amount of ΔE.

microcrystals and nanowires made of nitride-based semiconductors.[22,25,26] In our WZ/ZB/WZ structures, the lengths L_{ZB} of the ZB segments are much shorter than the lateral dimensions, resulting essentially in a simple parallel plate capacitor. Thus, the polarization sheet charge density σ can be estimated as[22,25]

$$\sigma = |P_{SP}| = \frac{\Delta V \varepsilon \varepsilon_0}{L_{ZB}}$$

where ΔV is the potential difference across the plate capacitor, ε is the dielectric constant of the material, and ε_0 is the permittivity of free space. The energy shift ΔE for changing the thickness of the capacitor with a single ZB monolayer is $\Delta E = \Delta V/q$, where q is the elementary charge. This relation results in a discrete red-shift (blue-shift) ΔE of the emission energy upon the addition (removal) of a single ZB monolayer.

Here, we demonstrate digital tuning of the GaP CPQW emission energy across a spectral range of 75 meV by varying the thickness of the ZB segment. The correlation between photoluminescence measurements and band structure simulations shows that the strong polarization field in GaP induces carrier confinement in the WZ section of the CPQW. The presence of atomically sharp interfaces results in emission line widths well below conventional III−V QW heterostructures. Therefore, the possibility to tailor the growth of WZ/ZB homojunctions in nanowires and thereby to digitally tune their emission energies provides a new tool in the design of solid-state

DOI: 10.1021/acs.nanolett.7b02489
Nano Lett. 2017, 17, 6062−6068

quantum emitters in small diameter nanowires featuring true QD emission.

In the WZ unit cell, the bond length between the Ga and P atoms along the ⟨0001⟩ axis (*c*-axis) is determined as a fraction *u* of the lattice parameter *c*, where *u* is called the internal cell parameter. In an ideal WZ unit cell with tetrahedral bonds, $u = 3/8 = 0.375$, and the resulting spontaneous polarization P_{SP} is equal to zero, which corresponds to the situation in the ZB unit cell. In WZ GaP nanowires, the measured value for the internal parameter is $u = 0.37385 \pm 0.00017$,[27] resulting in the prediction of a fairly large polarization $P_{SP}^{GaP} = 9\ mC/m^2$ along the *c*-axis. For comparison, calculations by density functional theory predict a value of $P_{SP}^{GaP} = 3\ mC/m^2$,[21] which is still higher than in other III−V semiconductors like GaAs, InAs, or InP, as summarized in Figure 1a.[21,27,28] Similarly, a significant spontaneous polarization with opposite sign ($u > 3/8$) is known from nitride-based materials.[21,22] As discussed above, the interface charges at the WZ/ZB/WZ junctions can be treated as a parallel plate capacitor to derive the polarization field responsible for the change in emission energy per monolayer (ML).[22] A more precise estimation of the evolution of the emission energy with ZB thickness can be performed using one-dimensional (1D) Schrödinger−Poisson calculations for the CPQWs along the *c*-axis (see Supporting Information S1 for more details).[29] We note that, as the exciton Bohr radius in GaP is smaller than 8 nm, no radial confinement is present in the 100 nm-thick nanowires.[19] In addition, the lattice mismatch between WZ and ZB structures is very small, and the piezoelectric field P_{PZ} is negligible compared to the spontaneous polarization field P_{SP}.[30] The type-I band profile for the WZ/ZB/WZ GaP structures calculated using the 1D Schrödinger−Poisson method is presented in Figure 1b,c. The calculated electron and hole wave functions depicted in Figure 1b show a small overlap due to the presence of the ZB barrier, which implies a longer carrier lifetime. The energy corresponding to this spatially indirect transition depends on the thickness of the ZB segment. Every addition of a ZB monolayer reduces the transition energy by an amount ΔE, as shown in Figure 1d, enabling digital tuning of the GaP CPQW emission lines.

For optical characterization of CPQWs, WZ GaP nanowires incorporating multiple defect-free WZ/ZB/WZ homojunctions with atomically sharp interfaces were investigated.[6] A representative WZ GaP nanowire of 100 nm diameter with multiple ZB segments is shown in the transmission electron microscopy (TEM) image in Figure 2a, where ZB sections with different lengths are separated by 200 nm long WZ segments. When considering the whole statistical ensemble of nanowires used for optical studies, ZB segments with lengths typically ranging between 3 and 60 MLs were investigated. As an example, ZB segments intentionally grown with lengths of 12 MLs and 33 MLs are shown in the high-resolution TEM (HRTEM) images in Figure 2b,c.

The optical emission of the CPQW is investigated using photoluminescence (PL) spectroscopy.[19,30,31] For this study, a high density of nanowires is dispersed on a SiO_x/Si substrate, and the optical emission is collected while scanning across the nanowire ensemble. Three different PL spectra of GaP nanowires with CPQWs are shown in Figure 3a, together with one PL spectrum from a pure WZ GaP nanowire. The α and γ peaks at 2.140 and 2.251 eV are related to bound excitons in WZ GaP,[19] whereas the additional sharp emission lines appear in a spectral region below the γ-line. This spectral region does not show any

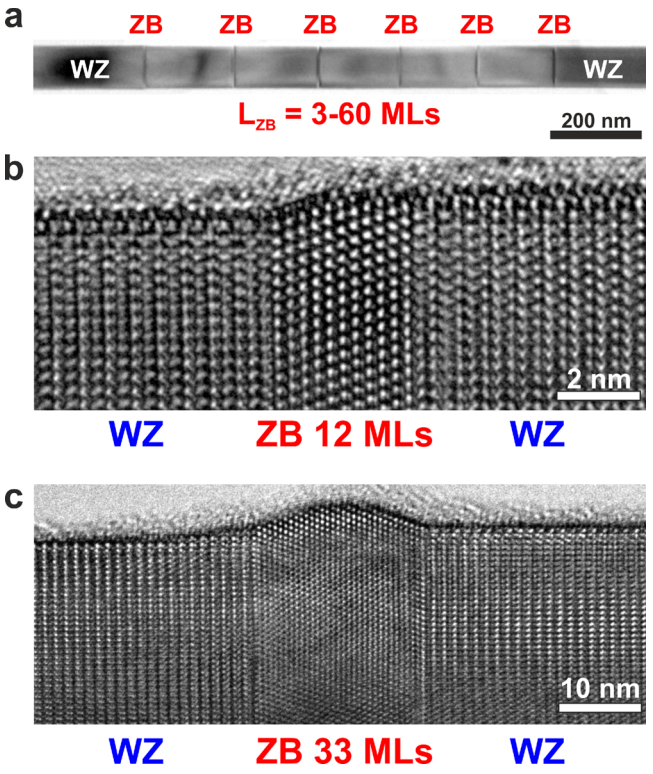

Figure 2. (a) TEM image of a WZ GaP nanowire with 100 nm diameter and multiple CPQWs of different ZB lengths separated by 200 nm long WZ segments. (b,c) HRTEM images of CPQWs with ZB segments of 12 MLs (b) and 33 MLs (c) in length.

emission lines in pure WZ GaP nanowires, clearly demonstrating that these peaks originate from the embedded CPQW segments. The CPQW emission lines show an average full width at half-maximum (fwhm) of 387 ± 13 μeV (see Figure 3b), reaching values as small as the setup resolution limit of about ∼200 μeV (see Supporting Information Figure S2). This line width is remarkably sharp for a III−V semiconductor QW and is the direct consequence of the presence of atomically sharp interfaces.[32] Once inhomogeneous broadening due to interface roughness is absent, the remaining broadening mechanism is due to charge fluctuations,[33] either due to nonresonant excitation in the CPQW barrier or due to charged impurities,which are unintentionally incorporated within the NW or at the NW surface. As a confirmation that the emission lines originate from the WZ sections of the CPQW, we performed polarization-dependent PL measurements on a single NW, as shown in the inset of Figure 3b. The emission from the CPQW is polarized perpendicular to the long nanowire *c*-axis ⟨0001⟩. This is in contrast to the isotropic behavior expected for carriers confined within a ZB GaP segment.[34,35] This observation strengthens the assumption of a type-I WZ/ZB junction with carrier confinement in the WZ segments, as predicted from band structure calculations.[12] A clear indication of the presence of different CPQWs in the PL spectra of Figure 3a is the regular spacing between multiple emission lines. To determine the emission energies of segments with a specific thickness in view of the variable emission energy, we performed a statistical analysis of the emission energy of hundreds of nanowires with CPQWs as summarized in the histogram in Figure 3c. Due to the occasional presence of the bound exciton β-line at 2.164 eV in WZ GaP,[19] the investigated energy range has been limited to 2.168−2.246

DOI: 10.1021/acs.nanolett.7b02489
Nano Lett. 2017, 17, 6062−6068

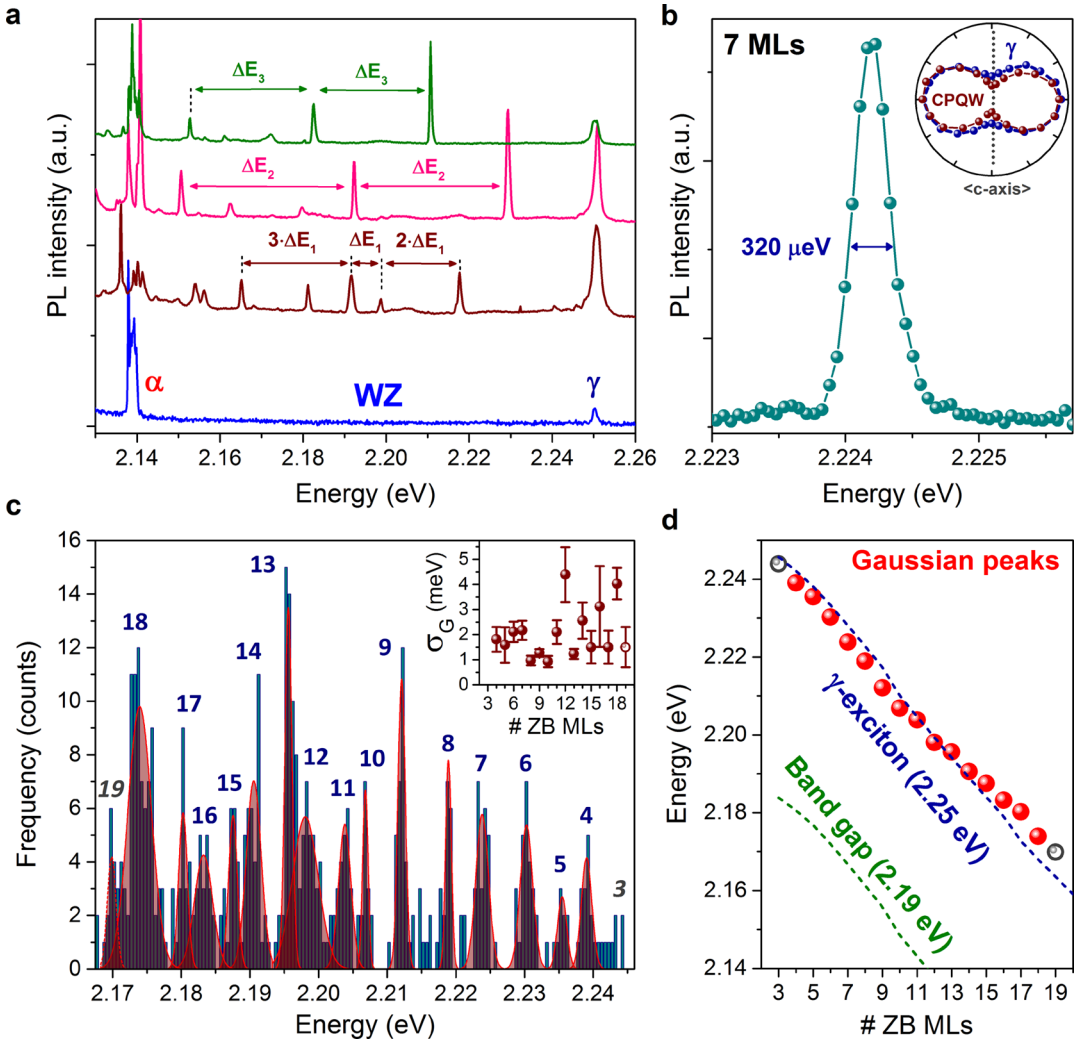

Figure 3. (a) PL spectra acquired for different CPQWs and compared with the emission from WZ GaP. (b) Enlarged view of a CPQW peak with a fwhm of ~320 μeV. Inset: polarization-dependent PL measurement on a single NW with CPQWs. (c) Statistical analysis of the emission energy of hundreds of nanowires with CPQWs. Fifteen Gaussian peaks are used for fitting, with additional peaks at 2.170 and 2.244 eV, with low statistical count being visible. A bin size of 0.5 meV is used for the histogram. Inset: width σ_G of the different Gaussian histogram peaks as a function of the ZB thickness. (d) Emission energy as a function of the number of ZB MLs (red spheres). The low statistical count peaks at 2.170 and 2.244 eV are indicated with hollow grey spheres. The 1D Poisson simulations using the WZ band gap of 2.19 eV (dashed dark green line) and γ-line bound exciton level at 2.25 eV (blue dashed line) are shown.

eV. Strikingly, from the multi-Gaussian peak fit of the histogram in Figure 3c, we observe up to 15 clear peaks, with additional peaks at 2.170 and 2.244 eV with low statistical counts. The presence of peaks in the histogram clearly shows that the CPQW emission lines are not random but instead exhibit a constant spacing of ~5 meV (see Figure 3d). This confirms that the position of the CPQW peaks is indeed governed by the respective number of ZB monolayers. Therefore, by tailoring the length of the ZB segments during growth,[6] CPQWs emitting at the same energy can be designed with a high degree of control. Since the shortest ZB segment in a WZ wire has a length of 3 MLs,[6] the first observable Gaussian peak should be associated with a ZB section of at least 3 MLs. The values for the standard deviation σ_G of the Gaussian peaks are in the range of 1−5 meV (inset Figure 3c). We tentatively explain the increased broadening of the histogram peak with increasing barrier thickness by a non-negligible number of charged impurities located within the ZB barrier at our background impurity concentration of 6×10^{17} cm^{-3} (see below). Charged impurities will locally change the confinement potential resulting in fluctuations of the emission energy, as reported for stacking faults in GaN[36] or InP QDs.[37] We note that the standard deviation of σ_G = 1−2 meV for the shorter segments is comparable to state-of-the-art QD samples[38] and probably can be further reduced by lowering the background impurity concentration.

The constant spacing of ~5 meV/ML is proportional with the polarization charge minus the compensating free charges due to background doping, which tend to accumulate near the ZB interface. For this reason, the energy shift per monolayer was calculated using the 1D Schrödinger−Poisson calculations as shown by the dashed line in Figure 3d. An unintentional background doping level of 6×10^{17} cm^{-3} as estimated from atom−probe tomography measurements on WZ GaP nanowires was considered in the model.[19] At this doping level, the calculations reproduce the experimentally observed trend for a spontaneous polarization of P_{SP} = 4.6 mC/m^2 (see Supporting Information S1 for more details). For a doping level of 1×10^{17}

DOI: 10.1021/acs.nanolett.7b02489
Nano Lett. 2017, 17, 6062−6068

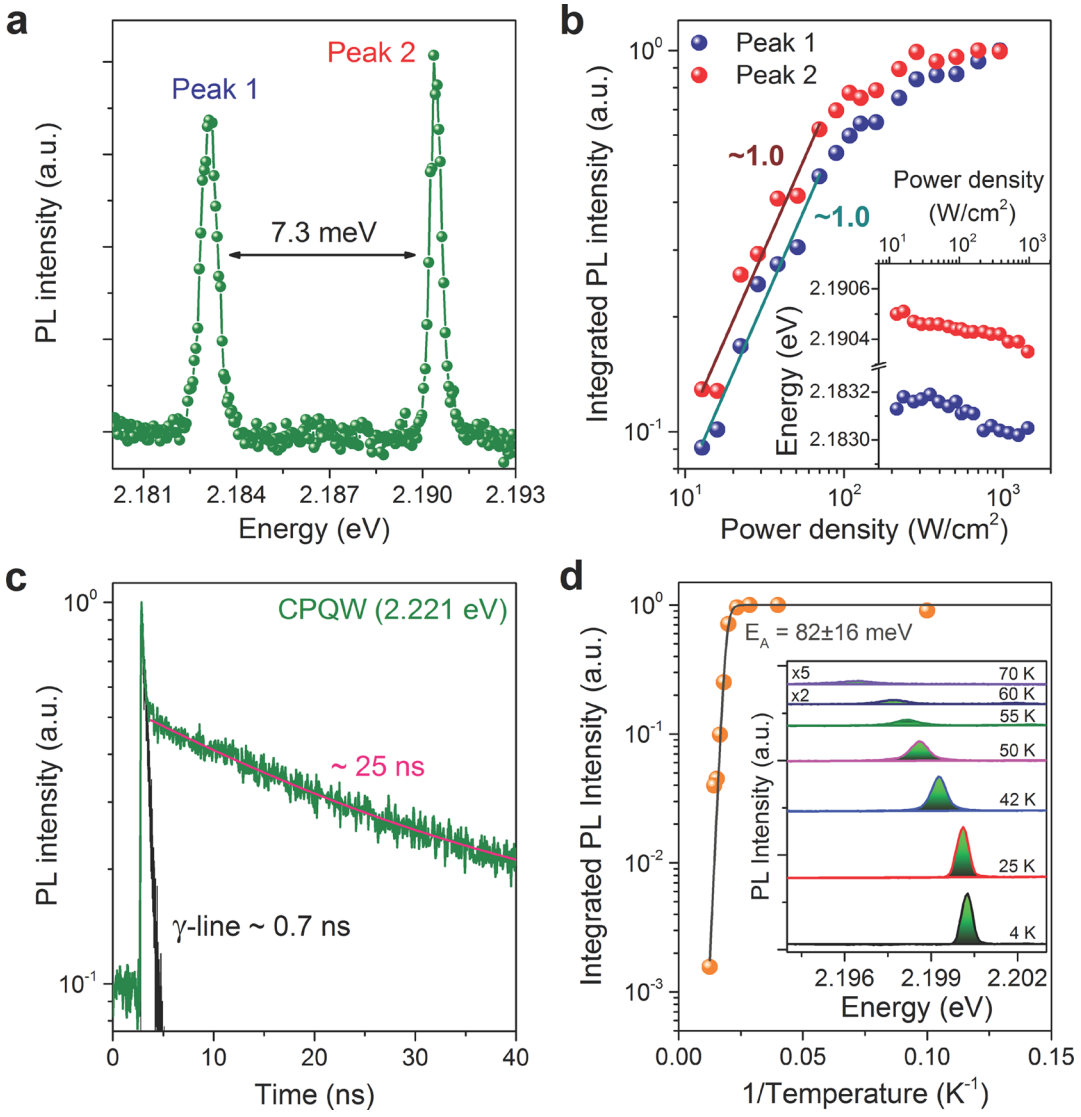

Figure 4. (a) PL spectra from two different QWs with a difference in thickness of 1 ZB ML. (b) Integrated PL intensity as a function of the excitation power density for the peaks in panel a. Inset: peak energy as a function of the excitation power density. (c) Time-resolved PL measurements on a CPQW peak at 2.221 eV compared with the time decay for the γ-exciton line. (d) Integrated PL intensity as a function of the reciprocal temperature for a CPQW at 2.220 eV. The fit is performed considering one active nonradiative recombination channel. Inset: PL spectra for increasing temperature.

(1×10^{18}) cm^{-3}, the experimental data would be reproduced for a polarization value of 2.8 (5.5) mC/m^2, which gives an estimate of the accuracy of the derived value. As the charge distribution due to doping is not taken into account, the plate capacitor approximation is not fully sufficient—in contrast to GaN, where the spontaneous polarization is 5 times larger.[22] A first calculation has been performed considering the WZ GaP bandgap of 2.19 eV, as shown by the green dashed line in Figure 3d.[19] However, despite the agreement with the trend of the experimental data, a clear offset in energy is present. Therefore, we performed a second calculation considering the γ-line bound exciton level at 2.25 eV for the WZ phase.[19] In this case, the resulting agreement with the experimental energies shows that the CPQW emission is related to a very efficient recombination channel associated with the localized γ-transition in WZ GaP. For comparison, the value we find for the spontaneous polarization P_{SP} is slightly higher than the 3 mC/m^2 predicted by DFT calculations,[21] but a factor of 2 lower than the estimate from the internal cell parameter u measured by X-ray diffraction.[27]

Power-dependent PL measurements were performed on emission lines at different energies to confirm that the emissions originate from different CPQWs. The two CPQW peaks in Figure 4a are separated by 7.3 meV, which differs from the expected shift of ~5 meV for the addition/removal of a ZB ML (see Figure 3d) possibly due to local fluctuations in doping concentrations. Looking at the excitation power dependence of the PL intensity as shown in Figure 4b, a linear scaling with slope ~1.0 is observed for both CPQW lines, followed by a saturation regime above 100 W/cm.[2] Furthermore, the absence of a blue-shift of the emission energy with increasing power (see inset Figure 4b) indicates that the number of photogenerated carriers is very small compared to the number of polarization charges, thus avoiding a blue shift due to compensation of the spontaneous polarization field by the photoinjected carriers. As a confirmation of the carrier separation in CPQWs, we performed time-resolved PL (TRPL) measurements, as shown in Figure 4c. The measured lifetime for different CPQW emission lines ranges between 20 and 30 ns. A clear correlation between increase in lifetime with increasing emission energy was

DOI: 10.1021/acs.nanolett.7b02489
Nano Lett. 2017, 17, 6062−6068

not observed. These values are much larger than the lifetime of 0.5−1.0 ns observed in WZ GaP in the same energy range and of the 0.70 ns lifetime for the γ-line.[19] Since the charge carriers are spatially separated and the transition is across a quantum barrier, the overlap of the electron and hole wave functions is reduced, which results in a decrease of the oscillator strength for the CPQW transition and hence in an increase of the radiative lifetime. However, we note that the presence of nonradiative recombination channels could affect the estimation of the lifetime from TRPL measurements, limiting our observations to a more qualitative picture. When the temperature of the system is increased, the emission from the CPQWs is quenched due to the thermal escape of holes out of the WZ confinement potential, as shown in Figure 4d. From fitting the temperature dependence of the integrated PL intensity of a CPQW at 2.200 eV using a single nonradiative recombination channel,[19] we find an activation energy $E_A = 82 \pm 16$ meV. In GaP, the WZ/ZB valence band offset is ∼135 meV (see Figure 1),[12] and considering the presence of quantized levels that reduce the energy barrier, the good agreement with E_A confirms the confinement of both electrons and holes in the WZ segment of the CPQW.

In this work, we have provided experimental evidence for the presence of a spontaneous polarization in WZ GaP, which has a strong effect on the optical properties of crystal phase homojunctions in this material system. We demonstrated digital tuning of the emission energy associated with WZ−ZB−WZ crystal phase quantum well structures by tailoring the length of the ZB segments. This approach will allow to grow crystal phase quantum dots (CPQDs) by decreasing the NW diameter, which is a step toward the controlled fabrication of multiple CPQDs emitting identical photons. Identical single photon emitters are a key ingredient for the realization of entangled states in quantum information processing.

■ ASSOCIATED CONTENT

Supporting Information

The Supporting Information is available free of charge on the ACS Publications website at DOI: 10.1021/acs.nanolett.7b02489.

Additional information on band structure calculations and optical characterization (PDF)

■ AUTHOR INFORMATION

Corresponding Author

*E-mail: j.e.m.haverkort@tue.nl.

ORCID

S. Assali: 0000-0002-3919-9112
J. Lähnemann: 0000-0003-4072-2369
K. D. Jöns: 0000-0002-5814-7510
L. Gagliano: 0000-0003-4214-8639
E. P. A. M. Bakkers: 0000-0002-8264-6862
J. E. M. Haverkort: 0000-0003-3051-673X

Present Addresses

[⊥]Department of Engineering Physics, Polytechnique Montréal, C. P. 6079, Succ. Centre-Ville, Montréal, Québec H3C 3A7, Canada.
[#]Applied Physics Department, Royal Institute of Technology, Albanova University Centre, Roslagstullsbacken 21, 106 91 Stockholm, Sweden.
[▽]Department of Photonics Engineering, Technical University of Denmark, 2800 Kongens Lyngby, Denmark.

Notes

The authors declare no competing financial interest.

■ ACKNOWLEDGMENTS

Maaike Bouwes Bavinck is acknowledged for the support in the PL measurements. This work was supported by the Dutch Organization for Scientific Research (NWO-VICI 700.10.441) and the Foundation for Fundamental Research on Matter (FOM). Solliance is acknowledged for funding the TEM facility.

■ REFERENCES

(1) Högele, A.; Seidl, S.; Kroner, M.; Karrai, K.; Warburton, R. J.; Gerardot, B. D.; Petroff, P. M. *Phys. Rev. Lett.* **2004**, *93* (21), 217401.
(2) Seidl, S.; Kroner, M.; Högele, A.; Karrai, K.; Warburton, R. J.; Badolato, A.; Petroff, P. M. *Appl. Phys. Lett.* **2006**, *88* (20), 203113.
(3) Bennett, A. J.; Pooley, M. A.; Stevenson, R. M.; Ward, M. B.; Patel, R. B.; de la Giroday, A. B.; Sköld, N.; Farrer, I.; Nicoll, C. A.; Ritchie, D. A.; Shields, A. J. *Nat. Phys.* **2010**, *6* (12), 947−950.
(4) Rastelli, A.; Ding, F.; Plumhof, J. D.; Kumar, S.; Trotta, R.; Deneke, C.; Malachias, A.; Atkinson, P.; Zallo, E.; Zander, T.; Herklotz, A.; Singh, R.; Křápek, V.; Schröter, J. R.; Kiravittaya, S.; Benyoucef, M.; Hafenbrak, R.; Jöns, K. D.; Thurmer, D. J.; Grimm, D.; Bester, G.; Dörr, K.; Michler, P.; Schmidt, O. G. *Phys. Status Solidi B* **2012**, *249* (4), 687−696.
(5) Aharonovich, I.; Englund, D.; Toth, M. *Nat. Photonics* **2016**, *10* (10), 631−641.
(6) Assali, S.; Gagliano, L.; Oliveira, D. S.; Verheijen, M. A.; Feiner, L.-F.; Plissard, S. R.; Bakkers, E. P. A. M. *Nano Lett.* **2015**, *15* (12), 8062−8069.
(7) Lehmann, S.; Jacobsson, D.; Dick, K. A. *Nanotechnology* **2015**, *26* (30), 301001.
(8) Loitsch, B.; Winnerl, J.; Grimaldi, G.; Wierzbowski, J.; Rudolph, D.; Morkötter, S.; Döblinger, M.; Abstreiter, G.; Koblmüller, G.; Finley, J. J. *Nano Lett.* **2015**, *15* (11), 7544−7551.
(9) Caroff, P.; Dick, K. A.; Johansson, J.; Messing, M. E.; Deppert, K.; Samuelson, L. *Nat. Nanotechnol.* **2009**, *4* (1), 50−55.
(10) Vainorius, N.; Lehmann, S.; Jacobsson, D.; Samuelson, L.; Dick, K. A.; Pistol, M.-E. *Nano Lett.* **2015**, *15* (4), 2652−2656.
(11) Akopian, N.; Patriarche, G.; Liu, L.; Zwiller, V. *Nano Lett.* **2010**, *10* (4), 1198−1201.
(12) Belabbes, A.; Panse, C.; Furthmüller, J.; Bechstedt, F. *Phys. Rev. B: Condens. Matter Mater. Phys.* **2012**, *86* (7), 75208.
(13) Dick, K. A.; Thelander, C.; Samuelson, L.; Caroff, P. *Nano Lett.* **2010**, *10* (9), 3494−3499.
(14) Bolinsson, J.; Caroff, P.; Mandl, B.; Dick, K. A. *Nanotechnology* **2011**, *22* (26), 265606.
(15) Bouwes Bavinck, M.; Jöns, K. D.; Zieliński, M.; Patriarche, G.; Harmand, J. C.; Akopian, N.; Zwiller, V. *Nano Lett.* **2016**, *16* (2), 1081−1085.
(16) Dean, P.; Thomas, D. *Phys. Rev.* **1966**, *150* (2), 690−703.
(17) Morgan, T. N. *Phys. Rev. Lett.* **1968**, *21* (12), 819−823.
(18) Bechstedt, F.; Belabbes, A. *J. Phys.: Condens. Matter* **2013**, *25* (27), 273201.
(19) Assali, S.; Greil, J.; Zardo, I.; Belabbes, A.; de Moor, M. W. A.; Koelling, S.; Koenraad, P. M.; Bechstedt, F.; Bakkers, E. P. A. M.; Haverkort, J. E. M. *J. Appl. Phys.* **2016**, *120* (4), 44304.
(20) Standing, A.; Assali, S.; Gao, L.; Verheijen, M. A.; van Dam, D.; Cui, Y.; Notten, P. H. L.; Haverkort, J. E. M.; Bakkers, E. P. A. M. *Nat. Commun.* **2015**, *6*, 7824.
(21) Belabbes, A.; Furthmüller, J.; Bechstedt, F. *Phys. Rev. B: Condens. Matter Mater. Phys.* **2013**, *87* (3), 35305.
(22) Lähnemann, J.; Brandt, O.; Jahn, U.; Pfüller, C.; Roder, C.; Dogan, P.; Grosse, F.; Belabbes, A.; Bechstedt, F.; Trampert, A.; Geelhaar, L. *Phys. Rev. B: Condens. Matter Mater. Phys.* **2012**, *86* (8), 081302.
(23) Fiorentini, V.; Bernardini, F.; Della Sala, F.; Di Carlo, A.; Lugli, P. *Phys. Rev. B: Condens. Matter Mater. Phys.* **1999**, *60* (12), 8849−8858.
(24) Miller, D. A. B.; Chemla, D. S.; Damen, T. C.; Gossard, A. C.; Wiegmann, W.; Wood, T. H.; Burrus, C. A. *Phys. Rev. Lett.* **1984**, *53* (22), 2173−2176.

DOI: 10.1021/acs.nanolett.7b02489
Nano Lett. 2017, 17, 6062−6068

(25) Lähnemann, J.; Jahn, U.; Brandt, O.; Flissikowski, T.; Dogan, P.; Grahn, H. T. *J. Phys. D: Appl. Phys.* **2014**, *47*, 423001.
(26) Hille, P.; Müßener, J.; Becker, P.; De La Mata, M.; Rosemann, N.; Magén, C.; Arbiol, J.; Teubert, J.; Chatterjee, S.; Schörmann, J.; Eickhoff, M. *Appl. Phys. Lett.* **2014**, *104*, 102104.
(27) Kriegner, D.; Assali, S.; Belabbes, A.; Etzelstorfer, T.; Holý, V.; Schülli, T.; Bechstedt, F.; Bakkers, E. P. A. M.; Bauer, G.; Stangl, J. *Phys. Rev. B: Condens. Matter Mater. Phys.* **2013**, *88* (11), 115315.
(28) Bauer, B.; Hubmann, J.; Lohr, M.; Reiger, E.; Bougeard, D.; Zweck, J. *Appl. Phys. Lett.* **2014**, *104* (21), 211902.
(29) Snider, G. 1D Poisson freeware; University of Notre Dame. http://www.nd.edu/~gsnider/ (accessed May 1, 2015).
(30) Greil, J.; Assali, S.; Isono, Y.; Belabbes, A.; Bechstedt, F.; Valega Mackenzie, F. O.; Silov, A. Y.; Bakkers, E. P. A. M.; Haverkort, J. E. M. *Nano Lett.* **2016**, *16* (6), 3703−3709.
(31) Assali, S.; Zardo, I.; Plissard, S.; Kriegner, D.; Verheijen, M. A.; Bauer, G.; Meijerink, A.; Belabbes, A.; Bechstedt, F.; Haverkort, J. E. M.; Bakkers, E. P. A. M. *Nano Lett.* **2013**, *13* (4), 1559−1563.
(32) Grundmann, M. *The Physics of Semiconductors*; Springer, 2006.
(33) Lodahl, P.; Mahmoodian, S.; Stobbe, S. *Rev. Mod. Phys.* **2015**, *87* (2), 347−400.
(34) Mishra, A.; Titova, L. V.; Hoang, T. B.; Jackson, H. E.; Smith, L. M.; Yarrison-Rice, J. M.; Kim, Y.; Joyce, H. J.; Gao, Q.; Tan, H. H.; Jagadish, C. *Appl. Phys. Lett.* **2007**, *91* (26), 263104.
(35) Wilhelm, C.; Larrue, A.; Dai, X.; Migas, D.; Soci, C. *Nanoscale* **2012**, *4* (5), 1446.
(36) Corfdir, P.; Lefebvre, P.; Ristić, J.; Ganière, J.-D.; Deveaud-Plédran, B. *Phys. Rev. B: Condens. Matter Mater. Phys.* **2009**, *80* (15), 153309.
(37) Reimer, M. E.; Bulgarini, G.; Fognini, A.; Heeres, R. W.; Witek, B. J.; Versteegh, M. A. M.; Rubino, A.; Braun, T.; Kamp, M.; Höfling, S.; Dalacu, D.; Lapointe, J.; Poole, P. J.; Zwiller, V. *Phys. Rev. B: Condens. Matter Mater. Phys.* **2016**, *93* (19), 195316.
(38) Juska, G.; Dimastrodonato, V.; Mereni, L. O.; Gocalinska, A.; Pelucchi, E. *Nat. Photonics* **2013**, *7*, 527−531.

DOI: 10.1021/acs.nanolett.7b02489
Nano Lett. 2017, 17, 6062−6068